

Cite this: DOI: 10.1039/c0xx00000x

www.rsc.org/xxxxxx

ARTICLE TYPE

Ligation of anti-cancer drugs to self-assembling ultrashort peptides by click chemistry for localized therapy

Michael R. Reithofer*, Kiat-Hwa Chan, Anupama Lakshmanan, Dang Hoang Lam, Archana Mishra, Began Gopalan, Mangesh Joshi, Shu Wang, and Charlotte A. E. Hauser*

5 Received (in XXX, XXX) XthXXXXXXXXXX 20XX, Accepted Xth XXXXXXXXXXXXX 20XX

DOI: 10.1039/b000000x

Self-assembling ultrashort peptides from aliphatic amino acids were functionalized with platinum anti-cancer drugs by click chemistry. Oxaliplatin-derived hybrid peptide hydrogels with up to 40% drug loading were tested for localized breast cancer therapy. Stably injected gels showed significant tumor growth inhibition in mice and a better tolerance compared to the free platinum drug.

10 Introduction

Self-assembly, the spontaneous organization of molecules into ordered structures by non-covalent interactions is the most fundamental process for building supramolecular structures^{1, 2} from DNA, proteins and other biomolecules in living systems.³ We have been able to harness the innate self-assembling capacity of rationally designed ultrashort peptides which contain only aliphatic amino acids.⁴⁻⁶ The self-assembly process of these ultrashort peptides has been addressed in detail and a hypothesis of the underlying mechanism has been discussed.⁴ In this study, we combine the use of these peptides as vehicles for sustained, local delivery of anti-cancer therapeutics and as scaffolds for replacing lost tissue and regenerating damaged tissue.

Platinum-based anticancer therapeutics are amongst the most widely used drugs in the clinics today for the treatment of different types of cancers. So far, three platinum(II) compounds have been approved by the FDA, namely cisplatin, carboplatin and oxaliplatin.⁷⁻¹⁰ These drugs are used against a number of solid tumors including prostate, breast, colorectal, non-small-cell lung, and genitourinary cancers.^{8, 11, 12} The drugs are administered intravenously, whereby only a small amount of the given dosage reaches the target.¹³ The majority of the drug is excreted and causes severe side effects ranging from nausea and ototoxicity to nephro- and neurotoxicity.¹⁴ Reducing side effects and enhancing drug uptake and efficacy is currently one of the biggest challenges in medicinal chemistry, especially in the development of metal based anti-cancer therapeutics.¹⁵⁻²⁵ Our aim is to address this challenge by using self-assembling ultrashort peptides as a platform for localized and sustained release of anti-cancer drugs.

Localized treatment, using *in situ* gelling delivery systems injected directly into the tumor site, is a feasible strategy to overcome systemic effects and poorly directed uptake. In addition, direct localized injection of a drug can be seen as a non-invasive therapeutic strategy, reducing hospitalization time and cost, thereby providing more comfort to patients. In case surgical removal of the tumor is required, such systems could be implanted

as biomimetic ECM supporting tissue regeneration, in combination with providing a localized therapeutic effect. For a number of malignancies localized treatment is already routine.²⁶⁻²⁸ Several polymer-based hydrogels are currently in development for localized drug delivery.²⁸⁻³² A major drawback of many synthetic polymeric hydrogels is the requirement of a crosslinking step that necessitates the use of potentially harmful agents such as organic solvents or chemical initiators. The residual presence of such agents decreases the biocompatibility of the hydrogels. On the other hand, UV-crosslinked polymers are often incompatible with many anticancer drugs (e.g. doxorubicin, daunorubicin, cyclophosphamide). Although hydrogels containing cisplatin directly coordinated to an amino acid have been reported, such systems often use an amino acid which is co-polymerized, yielding a hybrid peptide polymer system, where the drug is loaded after the polymerisation step. This results in poor solubility and does not offer the possibility of *in situ* gelation after a local injection.³³⁻³⁷

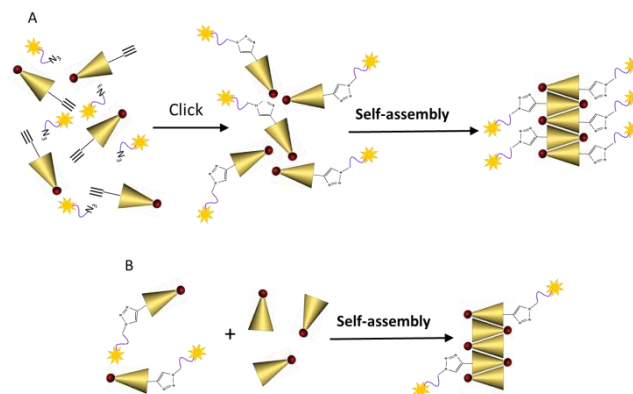


Fig. 1. Schematic drawing of a) peptide functionalization with a bioactive cue using click chemistry. The triangle represents the hydrophobic tail of the peptide showing decreasing lipophilicity from N- to C-terminus and the red dot represents the polar head group at the C-terminus; b) assembly of the parent peptide together with the functionalized ultrashort peptide, forming a hybrid system.

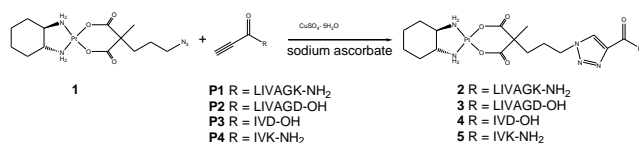
70 Natural biomolecules such as peptides, which self-assemble into

injectable hydrogels, offer a promising platform to overcome the above limitations. We recently reported a unique class of ultrashort peptides, which are able to form hydrogels by facile self-assembly without additional physico-chemical support or UV-crosslinking.^{4, 5}

The unique character of these ultrashort peptides and their biocompatibility afford them great potential as drug-delivery systems. Here, we report the synthesis and bioactivity of oxaliplatin-derived hybrid peptide hydrogels (Fig. 1). The ability of these ultrashort peptides to self-assemble into hydrogels, likely *via* an antiparallel mechanism, allows functionalization of the termini of the peptides without interfering with the self-assembling residue. Therefore, the functionalized peptide would still be able to assemble by itself or when mixed with its parent peptide, forming hybrid hydrogels (Fig. 1).

Results and discussion

A series of propiolic acid functionalized peptides, namely LIVAGK-NH₂, IVK-NH₂, LIVAGD-OH and IVD-OH were synthesized by standard Fmoc solid phase peptide synthesis. The N-terminus functionalization was performed on the solid phase-bound peptide, using HATU (*O*-(7-azabenzotriazolyl)-tetramethyluroniumhexafluorophosphate) as the coupling reagent without the addition of a base. The beads were washed after the coupling with a solution of 10% DIPEA (*N,N*-diisopropylethylamine) in DMF. The final coupling was repeated until a Kaiser test, (a ninhydrin based calorimetric assay which detects free amines of the resin-bound peptide),³⁸ detected no free amines. The alkyne residue allows for a fast and efficient derivatization of the peptides with bioactive cues via click chemistry. We chose an oxaliplatin derived precursor as the bioactive test compound. Here, 2-(3-azidopropyl)-2-methylmalonic acid was used as the biscalboxylato ligand yielding oxaliplatin analogues following standard synthetic protocols. The azide functionality on compound **1** allows the attachment to the alkyne functionalized peptide via a Cu(I) catalyzed 1,3-dipolar cycloaddition reaction, as shown in Scheme 1. The best yield was obtained when CuSO₄·5H₂O was reduced to Cu(I) *in situ* using sodium ascorbate, and H₂O/*t*BuOH/DMF in a ratio of 10:10:1 as the solvent (refer to ESI for details of synthesis and chemical characterization). The addition of DMF helped in solubilizing the starting compounds.



Scheme 1. Synthesis of oxaliplatin peptide conjugates.

The synthesized compounds were characterized in detail by multinuclear NMR (Fig. 2 and S2), FT-IR (Fig. S3 and S4), ESI-MS (Fig. S5, S6, S7 and S8) and UV-Vis spectroscopy (Fig. S9). For compound **2** and **4**, detailed structural analysis was carried out by multinuclear NMR experiments. The predicted structure of the

compounds could be clearly verified by 2D correlation experiments proving the success of the ligation reaction (Fig. 2, Fig. S2 for numbering scheme and ESI for complete assignment).

The successful click reaction could be verified by the characteristic ¹³C signals of the newly formed triazole ring at 127 (CH) and 141 (C_q) ppm respectively. Furthermore, the presence of the *1R,2R*-DACH ligand and its coordination to platinum can be proven by the characteristic proton resonance of the amine group (~5.5 ppm), which is shifted significantly to a lower field when coordinated to platinum. These experimental findings are in agreement with results obtained by ESI-MS and FT-IR spectroscopy. Additionally, the copper content in the final products (compound **2** and **4**) was quantified by ICP-MS. An insignificant copper content of less than 0.25 % was detected for compound **2** while for compound **4**, the copper content was below the detection limit of 10 ppb.

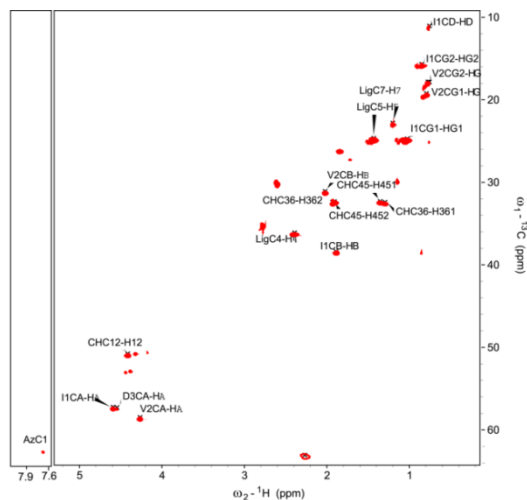


Fig. 2. ¹H,¹³C-HMQC NMR of compound **4**.

To test the gelation ability of compounds **2-5**, they were dissolved in water by vortexing and kept undisturbed overnight (Fig. 3). However, even at a concentration of 40 mg/mL, only clear solutions were obtained, and no hydrogel formation was observed. Interestingly, these peptide metal conjugates showed much higher water solubility than either oxaliplatin or cisplatin alone. In contrast, the alkyne-derived peptide **P1** gelled in water at a concentration of 29 mg/mL, which is close to the minimal gelation concentration of its parent peptide Ac-LIVAGK-NH₂ (Ac-LK₆-NH₂). Peptides **P2-P4** showed gelation behaviour similar to **P1**. We assume, that derivatization of the peptides with oxaliplatin and a bulky triazole group interferes with their self-assembly by changing the hydrophobic nature of the N-terminus of the peptide. However, stable hybrid gels could be formed with up to 40 wt% drug loading, when the parent peptide was used as a matrix. Since gelation time is critical for *in vivo* applications, the effect of peptide concentration on gelation time was investigated. In general, the gelation time can be easily adjusted by tuning the peptide concentration and type of solvent used. A faster gelation time is observed in PBS as compared to water for a given peptide concentration. Furthermore, the minimum concentration required for gelation is also lower in PBS buffer, which makes the system suitable for *in vivo* formulations.

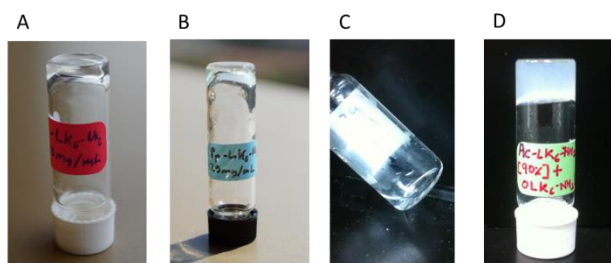


Fig. 3. Pictures of: A) Ac-LIVAGK-NH₂ at 25 mg/mL, B) peptide **P1** at 29 mg/mL C) solution of compound **2** at 40 mg/mL and D) co-gel containing 10 wt% of compound **2** and 90 wt% of Ac-LIVAGK-NH₂

Morphological characterization of the peptide hydrogel scaffolds was done by Field Emission Scanning Electron Microscopy (FESEM) and representative images for Ac-LIVAGK-NH₂, **P1** and **2** are shown in Fig.4. The three compounds showed similar morphologies that can be described as flat sheets and tapes with visible fibrous structures on the surface.

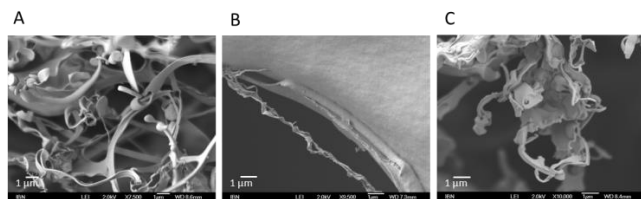


Fig. 4. Morphology of peptide hydrogels as imaged by FESEM. A) Ac-LIVAGK-NH₂ at 2 mg/mL, B) peptide **P1** at 29 mg/mL C) solution of compound **2** at 40 mg/mL

Cytotoxicity of all synthesized compounds was evaluated in two human cancer cell lines, namely HeLa (cervical carcinoma) and SW480 (colon carcinoma) cells. In addition, 4T1 mouse breast cancer cells were used. IC₅₀ values obtained by serial dilutions are listed in Table 1.

Table 1. Cytotoxicity values of platinum peptide conjugates **2-5** compared to cisplatin and oxaliplatin in three cancer cell lines.

Compound	IC ₅₀ [μM]		
	HeLa	SW480	4T1
2	4.4 ± 2.3	1.5 ± 0.8	2.9 ± 0.8
3	7.7 ± 1.4	1.5 ± 0.7	6.7 ± 0.9
4	3.4 ± 1.5	1.6 ± 1.1	2.1 ± 1.0
5	6.2 ± 1.3	2.3 ± 1.2	4.1 ± 1.0
Cisplatin	1.0 ± 0.8	4.0 ± 2.5	1.5 ± 0.6
Oxaliplatin	2.0 ± 0.8	0.47 ± 0.1	1.8 ± 0.5

The control compounds cisplatin and oxaliplatin exhibited IC₅₀ values in the sub-micromolar to low micromolar range in all three tested cell lines. Oxaliplatin showed the highest activity in SW480 cells whereas cisplatin was most active in HeLa cells. The same holds true for compound **2-5** with all compounds displaying the highest activity in SW480 cells (IC₅₀ = 1.5-2.3 μM) and least active in HeLa cells (IC₅₀ = 3.4-7.7 μM). To verify that the conjugation of

the compound **1** to the peptides does not significantly affect the cell cytotoxicity, its IC₅₀ value was also determined in HeLa cells. The resulting IC₅₀ value was within the expected range.

To further characterize the *in vitro* efficacy of compounds **2-5**, cell cycle analysis and caspase activity were evaluated. Specifically, we compared the response of SW480 and 4T1 cells to compounds **2-5**, and to the oxaliplatin control. All compounds induced an arrest in both cell lines in the G2/M phase, the checkpoint after DNA replication and preceding mitosis (see Fig. S12 and S13). Similar observations have been reported for the oxaliplatin control.³⁹ Oxaliplatin coordinates to DNA, preventing the cell from crossing the G2/M DNA damage check point. Although G2/M phase arrest of compounds **2-5** indicates, that compounds **2-5** are able to interact with DNA similarly to oxaliplatin, it is not a direct proof of DNA platination. For the SW480 cells, no apoptosis was observed with the oxaliplatin control as well as compounds **2-5**. However, relative to the untreated controls, the G1 phase was reduced and an increase in G2 (corresponding to a G2/M arrest) as well as in the S phase was seen for the test compounds. A significant increase in the G2 phase is observed for compounds **2-5**, majority of the cells were in the S phase. We attribute this to the ability of the compound to aggregate in solution, as well as specificity of the drug to a particular cell phenotype.

To further prove that the novel platinum-peptide conjugates are able to bind DNA, DNA platination on HeLa cells using compound **2** as the test compound and oxaliplatin as control were carried out (see ESI for experimental details). Isolated DNA was quantified and the platinum content of the samples were determined by ICP-MS. DNA platination was observed for both compound **2** as well as oxaliplatin, in which a DNA platination of 1.2 ± 0.03 pg platinum per μg DNA was found for compound **2** and 3.7 ± 0.7 pg platinum per μg DNA for oxaliplatin, respectively. The 3-fold increase in platination for oxaliplatin over compound **2** explains the slightly higher efficacy *in vitro* and *in vivo* for the oxaliplatin control, which is nevertheless countered by its detrimental effects such as poor tumor uptake and subsequently higher systemic toxicity (as indicated by *in vivo* results and biodistribution data).

By measuring caspase 3/7 activity, we confirmed that compounds **2-5** and the oxaliplatin control are able to induce apoptosis via the caspase 3/7 pathway. For all tested compounds, the highest caspase activity was detected at 10 μM after 72 h of incubation (see ESI for experimental details and Fig. S14 for time-dependent caspase 3/7 activity). In addition, compound **2** was used to examine the effects of concentration on caspase 3/7 activity (Fig. S15). No significant difference in caspase 3/7 activity was detected between SW480 and 4T1 cells. These results are in agreement with the cell cycle analysis, demonstrating the cytotoxicity of the oxaliplatin peptide conjugate.

Based on the promising *in vitro* efficacy of all tested oxaliplatin-derived compounds in 4T1 cells, we decided to evaluate the effect of a localised treatment in an *in vivo* mouse model.⁴⁰ Although compounds **2** and **4** showed similar IC₅₀ values, compound **2** was selected for *in vivo* evaluation due to the reduced acidity and lower gelation concentration of its parent peptide.

Female BALB/c mice were divided into four groups for treatment

(PBS group and Ac-LIVAGK-NH₂ hydrogel group as negative controls, oxaliplatin as positive control and test compound **2** as a hybrid hydrogel with Ac-LIVAGK-NH₂). Each group comprised 9 mice (see ESI for the experimental procedure). All compounds and controls were injected locally into the seven-day old tumor and reinjection was performed with half the dose on day 21.

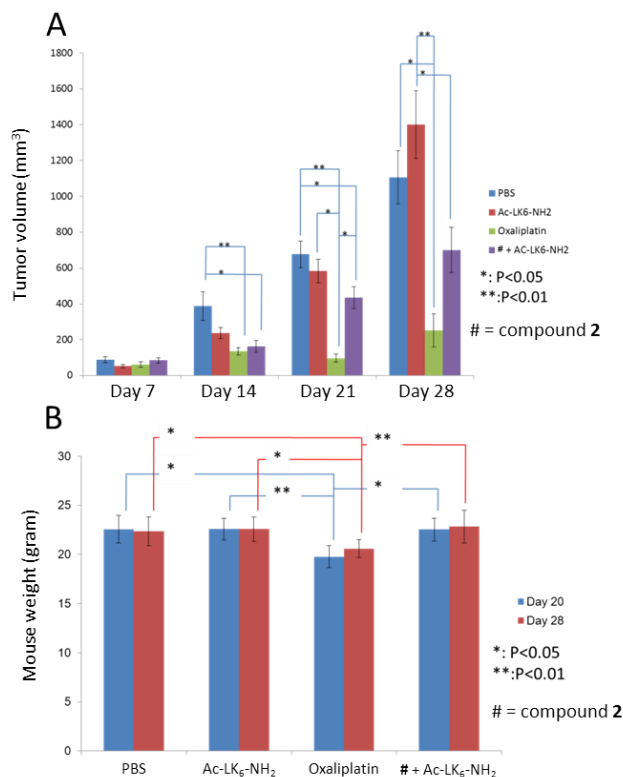


Fig. 5. Effects of oxaliplatin-derived peptide hybrid hydrogel in 4T1 tumor bearing mice. A) Tumor growth inhibition. BALB/c mice injected with 4T1 breast cancer cells (day 0) were divided into four groups to receive different treatments at day 7. Tumor volume measured at day 7, 14, 21, and 28 post tumor inoculation are shown (Mean \pm SE, n=9 per group). B) Reduced toxicity. Animals (n=9/group) were weighed at day 20 and 28 after tumor inoculation. For both measurements, one way ANOVA was performed (*: P<0.05, **: P<0.01).

Results of the tumor size measurements on day 7, day 14, day 21 and day 28 are shown in Fig. 5A. Statistical analysis was done using ANOVA to quantitatively discern significant differences among the groups for each time point based on tumor size (see ESI for the detailed statistical analysis). Significant tumor reduction was observed for the groups treated with oxaliplatin and compound **2**; seven and fourteen days post injection, in comparison with the PBS control group (Fig. 5A). Oxaliplatin displayed a greater effect on tumor size than compound **2**. However, oxaliplatin appeared to have a significant deleterious effect on the mice at the administered dose when compared to compound **2**. This was confirmed by a substantial weight difference between the oxaliplatin group and the group treated with compound **2** (Fig. 5B). Therefore, reinjection on day 21 involved only half the initial dose. On day 28, no statistically significant difference between the oxaliplatin group and the mice treated with **2** was found. However, the group treated with the hybrid hydrogel containing compound **2** showed a marked tumor growth inhibition when compared to the control group treated with the hydrogels alone (Fig. 5A). These results clearly

demonstrate the advantages of using this new drug delivery system for localized cancer treatment.

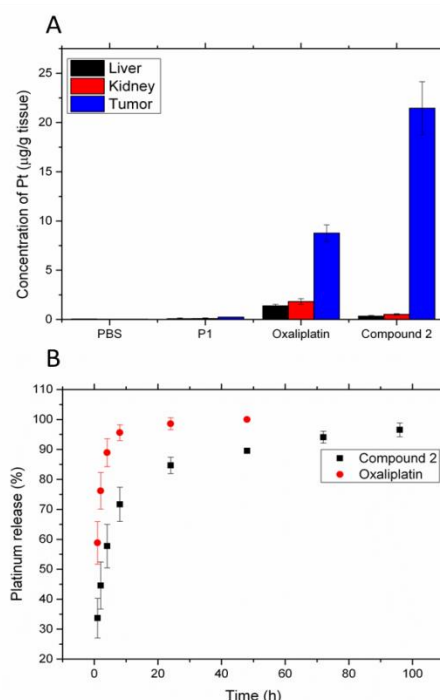


Fig. 6. Bio-distribution and drug release profiles (A) Bio-distribution profiles of the injected compounds in the liver, kidney and tumor of the treated animals. (B) *In vitro* drug release profile of the oxaliplatin-peptide conjugate and the free drug, in the presence of HeLa cells cultured in a 24-well transwell plate. Platinum concentration was measured using ICP-MS. At least three replicates were taken for each data point.

In order to further evaluate the *in vivo* efficacy and advantage of localized treatment using the hybrid oxaliplatin-peptide conjugate system, the tumor and other organs of the mice were isolated from the sacrificed animals at the end point of the therapy. Inductively coupled plasma mass spectrometry (ICP-MS) was used to analyze platinum (Pt) concentration in each organ (see ESI for experimental details). The bio-distribution of compound **2**, oxaliplatin, and the platinum-free controls (Ac-LIVAGK-NH₂ and PBS) are shown in Fig.6A. Enhanced tumor accumulation of compound **2** (21.5 µg/g tissue) was observed in the tumors treated with compound **2**, compared to the tumors that received oxaliplatin (8.8 µg/g tissue) alone (Fig. 6A). In the kidney and liver, which are the primary organs affected by oxaliplatin toxicity, compound **2** showed lower Pt levels (0.5 and 0.3 µg/g tissue) compared to the free oxaliplatin drug (1.8 and 1.4 µg/g tissue). The lower Pt levels in the liver and kidney confirm our earlier observations of reduced systemic toxicity of the conjugated drug compared to free oxaliplatin. To further establish the suitability of the novel platinum-peptide conjugate for injectable therapy and to elucidate the basis for the difference in tumor platinum concentration, the drug release kinetics was studied *in vitro*. For this purpose, drug release was quantified in the presence of HeLa cells (Fig.6B) over 4 days using a 24-well transwell plate setup (see ESI for experimental details). The drug release profile showed a significantly slower release for compound **2**. This effect is even more pronounced, when the same experiment is carried out in the absence of HeLa cells (Fig. S10A), resulting in approximately 80%

release of compound **2** after 4 days. Almost no changes were detected for the control oxaliplatin. **It has to be noted, that under the experimental condition, which are similar the conditions used for the cell cytotoxicity studies, the hydrogel does not disintegrate and has to be dissolved at the end of the study to determine the cumulative platinum release.** To further elucidate the release mechanism, a drug release study was carried out with a similar method to that used for the platinum release study (see ESI for experimental procedure). After 24 h of incubation at 37 °C the supernatant was analysed by HPLC-MS. The main compound identified was the parent peptide Ac-LK₆-NH₂, which is the major component of the co-gel. Compound **2** was also identified, together with released platinum. The fact that both Ac-LK₆-NH₂ and compound **2** were found can be explained through the dynamics of the self-assembly process, where at the interface between gel and solution, an equilibrium exists between the solubilised and gelled compound. As mentioned above, we also could identify platinum compounds with lower molecular weight, which can most likely be attributed to a released oxaliplatin compound which further reacts with the PBS buffer. To confirm that the observed compounds are the result of a reaction between the free platinum compound and the PBS buffer, [PtI₂(DACH)] was activated with AgNO₃ and added to PBS buffer. After analysis, the same molecular weight as for the hydrogel sample was seen. The above observation supports our initial working hypothesis - i.e. the peptide moiety of the platinum-peptide conjugate functions as an anchor group within the hydrogel scaffold of the parent peptide; and thus enables a more controlled release.

Conclusions

In conclusion, we have successfully functionalized the self-assembling ultrashort peptides with platinum anti-cancer drugs by click chemistry. The synthetic strategy is a general approach and can be used to attach a variety of bioactive molecules. Through extensive *in vitro* and *in vivo* evaluations, we show that the functionalized peptides can be used for localized cancer therapy using its parent peptide as the matrix. The peptide residue of compound **2-5**, when mixed with its parent peptide, is stably integrated into the hydrogel. All peptide compounds showed promising *in vitro* and *in vivo* activity. More importantly, the oxaliplatin-peptide conjugates displayed significantly lower systemic toxicity and higher localization in the target tissue compared to the free drug. We are currently exploring the use of ultrashort peptides as carriers for controlled release of doxorubicin and other cytostatics, where the release is controlled through a pH or light-sensitive linker. In summary, the use of hybrid peptide hydrogels containing anti-cancer drugs offers promising alternatives for current anti-cancer therapies, by enabling more efficient localized treatment and providing additional support as a 3D-scaffold for lost or damaged tissue.

Acknowledgements

This work is funded by the Institute of Bioengineering and Nanotechnology (Biomedical Research Council, Agency for Science, Technology and Research, Singapore).

Notes and references

Institute of Bioengineering and Nanotechnology, 31 Biopolis Way, The Nanos, Singapore 138669, Singapore Fax: (65)-6478-9080; phone: (+65)-6824-7108; e-mail: chauser@ibn.a-star.edu.sg, mreithofer@ibn.a-star.edu.sg

† Electronic Supplementary Information (ESI) available: Experimental materials and methods and characterization details of all compounds. See DOI: 10.1039/b000000x/

1. J.-M. Lehn, *Science*, 2002, **295**, 2400-2403.
2. G. M. Whitesides and B. Grzybowski, *Science*, 2002, **295**, 2418-2421.
3. C. M. Dobson, *Nature*, 2003, **426**, 884-890.
4. C. A. E. Hauser, R. Deng, A. Mishra, Y. Loo, U. Khoe, F. Zhuang, D. W. Cheong, A. Accardo, M. B. Sullivan, C. Riekel, J. Y. Ying and U. A. Hauser, *Proc. Natl. Acad. Sci. USA*, 2011, **108**, 1361-1366.
5. A. Mishra, Y. Loo, R. Deng, Y. J. Chuah, H. T. Hee, J. Y. Ying and C. A. E. Hauser, *Nano Today*, 2011, **6**, 232-239.
6. A. Lakshmanan and C. A. E. Hauser, *Int. J. Mol. Sci.* 2011, **12**, 5736-5746.
7. J. Graham, M. Muhsin and P. Kirkpatrick, *Nat. Rev. Drug. Discov.* 2004, **3**, 11-12.
8. L. Kelland, *Nat. Rev. Cancer*, 2007, **7**, 573-584.
9. B. Rosenberg, L. Van Camp and T. Krigas, *Nature*, 1965, **205**, 698-699.
10. B. Rosenberg, L. Vancamp, J. E. Trosko and V. H. Mansour, *Nature*, 1969, **222**, 385-386.
11. A. Horwich, J. Shipley and R. Huddart, *The Lancet*, **367**, 754-765.
12. H. M. Keys, B. N. Bundy, F. B. Stehman, L. I. Muderspach, W. E. Chafe, C. L. Suggs, J. L. Walker and D. Gersell, *N. Engl. J. Med.* 1999, **340**, 1154-1161.
13. D. Wang and S. J. Lippard, *Nat. Rev. Drug. Discov.* 2005, **4**, 307-320.
14. P. J. O'Dwyer, J. P. Stevenson and S. W. Johnson, *Drugs*, 2000, **59**, 19-27.
15. S. Dhar, F. X. Gu, R. Langer, O. C. Farokhzad and S. J. Lippard, *Proc. Natl. Acad. Sci. USA*, 2008, **105**, 17356-17361.
16. N. Graf and S. J. Lippard, *Adv. Drug Deliver. Rev.* 2012, **64**, 993-1004.
17. M. Galanski and B. K. Keppler, *Anticancer Agents Med. Chem.* 2007, **7**, 55-73.
18. M. R. Reithofer, A. K. Bytzek, S. M. Valiahd, C. R. Kowol, M. Groessl, C. G. Hartinger, M. A. Jakupec, M. Galanski and B. K. Keppler, *J. Inorg. Biochem.* 2011, **105**, 46-51.
19. M. R. Reithofer, S. M. Valiahd, M. A. Jakupec, V. B. Arion, A. Egger, M. Galanski and B. K. Keppler, *J. Med. Chem.* 2007, **50**, 6692-6699.
20. M. R. Reithofer, A. Schwarzing, S. M. Valiahd, M. Galanski, M. A. Jakupec and B. K. Keppler, *J. Inorg. Biochem.* 2008, **102**, 2072-2077.
21. R. P. Feazell, N. Nakayama-Ratchford, H. Dai and S. J. Lippard, *J. Am. Chem. Soc.* 2007, **129**, 8438-8439.
22. S. Dhar, Z. Liu, J. r. Thomale, H. Dai and S. J. Lippard, *J. Am. Chem. Soc.* 2008, **130**, 11467-11476.
23. S. Dhar, N. Kolishetti, S. J. Lippard and O. C. Farokhzad, *Proc. Natl. Acad. Sci. USA*, 2011, **108**, 1850-1855.
24. S. Dhar, W. L. Daniel, D. A. Giljohann, C. A. Mirkin and S. J. Lippard, *J. Am. Chem. Soc.* 2009, **131**, 14652-14653.

-
25. J. Li, S. Q. Yap, C. F. Chin, Q. Tian, S. L. Yoong, G. Pastorin and W. H. Ang, *Chem. Sci.* 2012, **3**, 2083-2087.
26. H. Brem, S. Piantadosi, P. C. Burger, M. Walker, R. Selker, N. A. Vick, K. Black, M. Sisti, S. Brem, G. Mohr, P. Muller, R. Morawetz and S. C. Schold, *The Lancet*, 1995, **345**, 1008-1012.
- 5 27. M. Westphal, Z. Ram, V. Riddle, D. Hilt and E. Bortey, *Acta Neurochir.* 2006, **148**, 269-275.
28. G. Fiorentini, C. Aliberti, M. Tilli, L. Mulazzani, F. Graziano, P. Giordani, A. Mambrini, F. Montagnani, P. Alessandroni, V. Catalano, P. Coschiera, P. *Anticancer Res.* **2012**, *32*, 1387-1395.
- 10 29. A. M. Al-Abd, K.-Y. Hong, S.-C. Song and H.-J. Kuh, *J. Control. Rel.* 2010, **142**, 101-107.
30. G. Chang, T. Ci, L. Yu and J. Ding, *J. Control. Rel.* 2011, **156**, 21-27.
- 15 31. J. B. Wolinsky, R. Liu, J. Walpole, L. R. Chirieac, Y. L. Colson and M. W. Grinstaff, *J. Control. Rel.* 2010, **144**, 280-287.
32. F. P. Seib, E. M. Pritchard and D. L. Kaplan, *Adv. Funct. Mater.* 2012, *23*, 58-65.
33. M. Casolaro, D. B. Barbara and M. Emilia, *Colloids Surf. B. Biointerfaces*, 2011, **88**, 389-395.
- 20 34. M. Casolaro, R. Cini, B. Del Bello, M. Ferrali and E. Maellaro, *Biomacromolecules*, 2009, **10**, 944-949.
35. J. R. Tauro and R. A. Gemeinhart, *Mol. Pharm.* 2005, **2**, 435-438.
36. J. R. Tauro and R. A. Gemeinhart, *Bioconjugate Chem.* 2005, **16**, 1133-1139.
- 25 37. J. R. Tauro, B.-S. Lee, S. S. Lateef and R. A. Gemeinhart, *Peptides*, 2008, **29**, 1965-1973.
38. E. Kaiser, R. L. Colescott, C. D. Bossinger and P. I. Cook, *Anal. Biochem.* 1970, **34**, 595-598.
- 30 39. S. William-Faltaos, D. Rouillard, P. Lechat and G. Bastian, *Fundam. Clin. Pharmacol.* 2007, **21**, 165-172.
40. A. Paraskar, S. Soni, B. Roy, A. L. Papa and S. Sengupta, *Nanotechnology*, 2012, **23**, 075103/1-075103/9.

35